

## Signatures of diradicals in X-ray absorption spectroscopy

Kevin Marin,<sup>1</sup> Meng Huang,<sup>1</sup> and Francesco A. Evangelista<sup>1, a)</sup>

*Department of Chemistry and Cherry Emerson Center for Scientific Computation,  
Emory University, Atlanta, Georgia, 30322, U.S.A.*

5

(Dated: 7 March 2023)

Theoretical simulations are critical to analyze and interpret the X-ray absorption spectrum of transient open-shell species. In this work, we propose a model of the many-body core-excited states of symmetric diradicals. We apply this model to analyze the carbon K-edge transitions of *o*-, *m*-, and *p*-benzyne, three organic diradicals with diverse and unusual electronic structures. The predictions of our model are compared with high-level multireference computations of the K-edge spectrum of the benzyne obtained with the driven similarity renormalization group truncated to third order. Our model shows the importance of a many-body treatment of the core-excited states of the benzyne and provides a theoretical framework to understand which properties of the ground state of these diradicals can be extracted from their X-ray spectrum.

10

15

---

<sup>a)</sup>Electronic mail: francesco.evangelista@emory.edu

## I. INTRODUCTION

The recent advent of intense and tunable sources of X-rays has made absorption spectroscopy of core electrons an invaluable tool to probe the local structure and dynamics of molecules and materials with element- and site-specificity.<sup>1,2</sup> Near-edge X-ray absorption fine structure (NEXAFS) spectroscopy probes transitions of core electrons to valence levels producing quasi-bound states. NEXAFS spectra (particularly the pre-edge region) are sensitive to changes in electronic structure and molecular geometry and can therefore provide new information not available from other spectroscopies.

From an independent-particle perspective, the molecular core-excited states probed in NEXAFS can be modeled as one-electron transitions from core to unoccupied levels, with the remaining spectator occupied orbitals kept frozen. The most important correction to this picture is orbital relaxation (rehybridization) due to the change in effective nuclear charge experienced by valence and unoccupied levels, a fundamental ingredient in many quantum chemistry methods for simulating NEXAFS spectra.<sup>3–7</sup>

This independent-particle approximation often breaks down for core excitations that involve multiple electrons or when the final state displays a complex many-body structure resulting from orbital near-degeneracies, such as in open-shell species.<sup>8–14</sup> In these cases, the accurate simulation of X-ray absorption spectra becomes challenging as it is necessary to explicitly account for the mixing of multiple electron configurations of excitation rank beyond one. Furthermore, the break down of the independent-particle approximation complicates the interpretation of NEXAFS spectra. For example, although this picture supports the interpretation of transition intensities as probes of orbital occupation and covalency (e.g., as discussed by Neese *et al.*<sup>15</sup>), strong many-body interactions resulting from the near-degeneracy of valence orbitals can result in significant configuration mixing.<sup>16</sup> As a result, it might become challenging to bridge the ground-state electronic structure of open-shell molecules and features of their NEXAFS spectra.

## II. MODEL

In this Communication, we propose a model to interpret the fundamental features of the NEXAFS spectrum of diradicals, which we apply to analyze, as a prototypical example, the carbon K-edge spectrum of *o*-, *m*-, and *p*-benzyne (shown in Fig. 1). The benzyne are prominent examples of organic diradicals<sup>17,18</sup> and display increasing open-shell character (due to orbital near-

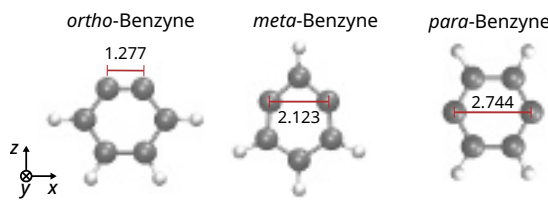


FIG. 1. Molecular structure and orientation of the three isomers of benzene optimized at the all-electron CCSD(T)/cc-pCVDZ level of theory. The distance between radical centers is given in angstrom.

degeneracy) from the *ortho* to the *para* isomer. They have been studied both experimentally<sup>19–24</sup> and theoretically,<sup>25–32</sup> providing a potential target for future NEXAFS measurements. Our model is employed to interpret the NEXAFS spectra of the benzenes computed with a high-level treatment of electron correlation using the recently proposed generalized-active-space multireference driven similarity renormalization group (GAS-MR-DSRG) framework.<sup>13,33</sup>

The model we consider consists of a diradical with unpaired electrons centered on atoms A and B, as shown in Fig. 2A. We assume that the radical centers A and B are equivalent; however, it is not difficult to generalize the present treatment to two inequivalent sites. The core orbitals localized on A and B are indicated with  $1s_A$  and  $1s_B$ , while the valence radical centers (partially occupied in the ground state) are indicated with  $\psi_A$  and  $\psi_B$ . The present model shares some similarities with models of the charge-transfer problem<sup>34,35</sup> and singlet-triplet fission.<sup>36</sup> Without loss of generality, we assume that the ground state of the diradical is a singlet. The dominant contribution to the ground state of the diradical is the covalent configuration

$$|\Phi_C\rangle = |(1s_A)^2(1s_B)^2(\psi_A)^1(\psi_B)^1\rangle, \quad (1)$$

where, for clarity, we omit to show the remaining doubly occupied spectator orbitals. Note that this configuration may represent either a singlet or a triplet state, depending on the spin coupling of the unpaired electrons, and in general it is the sum of several determinants. For a singlet state, we also account for the zwitterionic configuration

$$|\Phi_Z\rangle = \frac{1}{\sqrt{2}} \left( |(1s_A)^2(1s_B)^2(\psi_A)^2\rangle + |(1s_A)^2(1s_B)^2(\psi_B)^2\rangle \right). \quad (2)$$

Therefore, the diradical singlet ground state ( $\Psi_{\text{gs}}^S$ ) can be written as  $|\Psi_{\text{gs}}^S\rangle = C_C |\Phi_C\rangle + C_Z |\Phi_Z\rangle$ , where the coefficients  $C_C$  and  $C_Z$  determine the mixing of the covalent and zwitterionic configurations.

Core-excited states resulting from all possible  $1s \rightarrow \psi$  transitions, can be represented in a basis of eight determinants, as shown in Fig. 2B. Four determinants correspond to local excitations (LE)

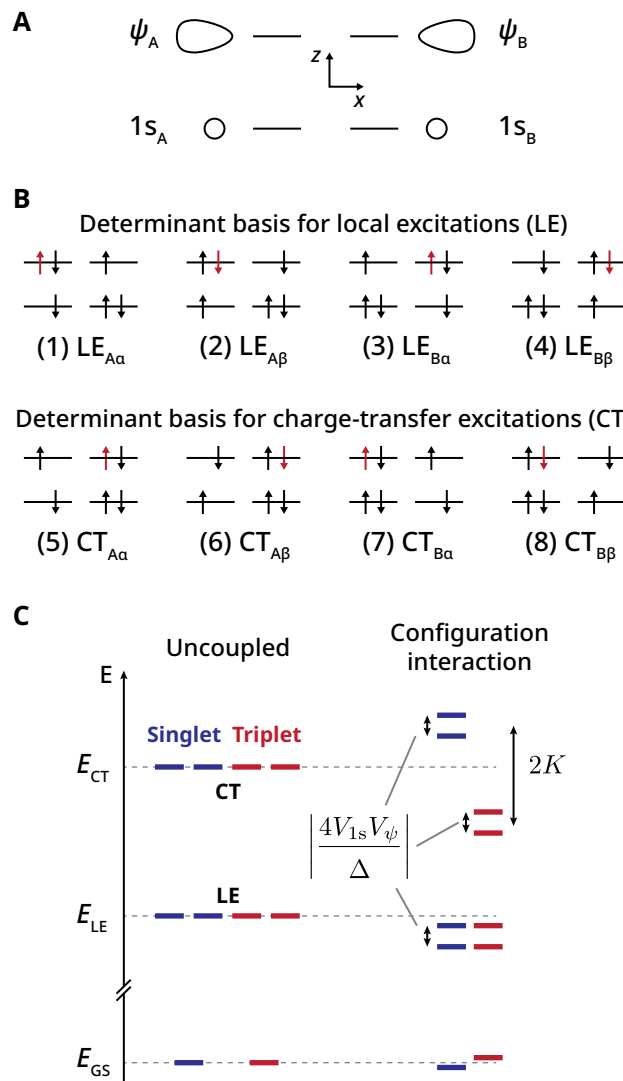


FIG. 2. Model of the core-excited states of a diradical with equivalent centers A and B. (A) Localized 1s core ( $1s_A$ ) and radical ( $\psi$ ) orbitals. (B) Determinant basis for local (LE) and charge-transfer (CT) core-excited states. (C) Energy of the singlet and triplet ground state determinants (GS) and LE/CT core-excited basis ignoring any coupling (“uncoupled”) and after coupling (“configuration interaction”).

(e.g.,  $1s_A \rightarrow \psi_A$ ) and arise from the following electron configurations  $(1s_A)^1(1s_B)^2(\psi_A)^2(\psi_B)^1$  and  $(1s_A)^2(1s_B)^1(\psi_A)^1(\psi_B)^2$ . The remaining four determinants are charge-transfer (CT) excitations (e.g.,  $1s_A \rightarrow \psi_B$ ) and arise from the electron configurations  $(1s_A)^1(1s_B)^2(\psi_A)^1(\psi_B)^2$  and  $(1s_A)^2(1s_B)^1(\psi_A)^2(\psi_B)^1$ . These eight determinants span a space of four singlet and four triplet states ( $M_S = 0$  component).

The matrix representation of the electronic Hamiltonian operator ( $\mathbf{H}$ ) in the basis of core-excited

states has the following structure:

$$\mathbf{H} = \begin{pmatrix} E_{\text{LE}} & 0 & 0 & 0 & V_{\psi} & 0 & V_{1s} & 0 \\ 0 & E_{\text{LE}} & 0 & 0 & 0 & V_{\psi} & 0 & V_{1s} \\ 0 & 0 & E_{\text{LE}} & 0 & V_{1s} & 0 & V_{\psi} & 0 \\ 0 & 0 & 0 & E_{\text{LE}} & 0 & V_{1s} & 0 & V_{\psi} \\ V_{\psi} & 0 & V_{1s} & 0 & E_{\text{CT}} & K & 0 & 0 \\ 0 & V_{\psi} & 0 & V_{1s} & K & E_{\text{CT}} & 0 & 0 \\ V_{1s} & 0 & V_{\psi} & 0 & 0 & 0 & E_{\text{CT}} & K \\ 0 & V_{1s} & 0 & V_{\psi} & 0 & 0 & K & E_{\text{CT}} \end{pmatrix}. \quad (3)$$

75 The diagonal entries of  $\mathbf{H}$  are energies of the LE and CT determinants ( $E_{\text{LE}}/E_{\text{CT}}$ ). Many of the off-diagonal elements of  $\mathbf{H}$  are given by integrals over molecular orbitals on both radical centers A and B, and are negligible due to small spatial overlap.

80 The nonzero elements of  $\mathbf{H}$  can be related to matrix elements of a Fock-like one-electron operator,  $f_{ij} = \langle \phi_i | \hat{f} | \phi_j \rangle$ , and two-electron integrals  $\langle \phi_i \phi_j | \phi_k \phi_l \rangle = \int d\mathbf{r}_1 d\mathbf{r}_2 \phi_i(\mathbf{r}_1) \phi_j(\mathbf{r}_2) r_{12}^{-1} \phi_k(\mathbf{r}_1) \phi_l(\mathbf{r}_2)$ , where  $\phi_i$  stands for any of the four localized spatial orbitals. The exchange integral  $K = -\langle 1s_A \psi_A | \psi_A 1s_A \rangle = -\langle 1s_B \psi_B | \psi_B 1s_B \rangle$  couples CT determinants connected by the exchange of two electrons on the same radical center (e.g.,  $|\text{CT}_{A\alpha}\rangle$  and  $|\text{CT}_{A\beta}\rangle$ ). Due to the local nature of  $K$  (i.e., all orbitals are on either A or B), its magnitude is expected to be similar for different diradicals. The one-electron integral  $V_{\psi} = \langle \psi_A | \hat{f} | \psi_B \rangle$  couples LE and CT determinants connected by the excitation  $\psi_A \rightarrow \psi_B$  (e.g.,  $|\text{LE}_{A\alpha}\rangle$  and  $|\text{CT}_{A\alpha}\rangle$ ). Similarly,  $V_{1s} = \langle 1s_A | \hat{f} | 1s_B \rangle$ , couples determinants that differ in the occupation of 1s orbitals on different centers. In the systems we considered,  $K$  and  $V_{\psi}$  are typically the off-diagonal elements of  $\mathbf{H}$  with the largest magnitude. Both  $V_{\psi}$  and  $V_{1s}$  depend on the separation between the radical centers; in practice, for the benzenes only  $V_{\psi}$  varies significantly, while  $V_{1s}$  is nearly constant and 5–20 times smaller than the former.

85 90 Once projected onto the manifold of singlet core-excited states, the Hamiltonian reduces to

$$\mathbf{H}^{S=0} = \begin{pmatrix} E_{\text{LE}} & 0 & V_{\psi} & V_{1s} \\ 0 & E_{\text{LE}} & V_{1s} & V_{\psi} \\ V_{\psi} & V_{1s} & E_{\text{CT}} + K & 0 \\ V_{1s} & V_{\psi} & 0 & E_{\text{CT}} + K \end{pmatrix}. \quad (4)$$

The eigenvalues of  $\mathbf{H}^{S=0}$  are given by

$$E_S = E_{\text{LE}} + \frac{1}{2} \left( \Delta_S \pm \sqrt{\Delta_S^2 + 4(V_{\psi} \pm V_{1s})^2} \right), \quad (5)$$

where  $\Delta_S = E_{CT} + K - E_{LE}$  is the difference between the energy of the CT and LE singlet states (and generally,  $\Delta_S > 0$ ) and the “ $\pm$ ” are taken independently (i.e., giving rise to four distinct eigenvalues). For the systems considered in this work,  $\Delta_S$  is larger than the magnitude of  $V_\psi \pm V_{1s}$  and the singlet states preserve their LE and CT character. Two states have local excitation character and their energy is approximately equal to

$$E_{LE,\pm}^S \approx E_{LE} - \frac{(V_\psi \pm V_{1s})^2}{\Delta_S}, \quad (6)$$

while two states have charge-transfer character and the following energies

$$E_{CT,\pm}^S \approx E_{CT} + K + \frac{(V_\psi \pm V_{1s})^2}{\Delta_S}. \quad (7)$$

One may similarly project the Hamiltonian onto the triplet manifold and express the eigenvalues for the LE states approximately as

$$E_{LE,\pm}^T \approx E_{LE} - \frac{(V_\psi \pm V_{1s})^2}{\Delta_T}, \quad (8)$$

where  $\Delta_T = E_{CT} - K - E_{LE}$  is the difference between the energy of the CT and LE triplet states. The two charge-transfer states have the following energies

$$E_{CT,\pm}^T \approx E_{CT} - K + \frac{(V_\psi \pm V_{1s})^2}{\Delta_T}. \quad (9)$$

In summary, as shown in Fig. 2C, the main effect of the interaction among the four singlet and triplet states is the splitting of the singlet and triplet CT states by a factor  $2K$ . The one-electron terms  $V_\psi$  and  $V_{1s}$  are responsible for splitting the double degeneracy within each group of LE and CT states by a factor of approximately  $4V_\psi V_{1s}/\Delta$ .

Lastly, we discuss the transition dipole moments when starting from the lowest singlet or triplet state. The transition moments may be expressed in terms of dipole integrals for a local excitation ( $\mu_{LE} = \langle 1s_A | \hat{\mu} | \psi_A \rangle$ ) and a charge-transfer excitation ( $\mu_{CT} = \langle 1s_A | \hat{\mu} | \psi_B \rangle$ ), where  $|\mu_{LE}| \gg |\mu_{CT}|$  due to the smaller overlap of the core and  $\sigma_{rad}$  orbitals in the CT case. Equations for the transition dipole moments of our model obtained by a first-order approximation of the eigenvectors are reported in Tab. S1 of the Supplementary Material. The model here takes advantage of the symmetry of the benzenes, and only the  $x$  and  $z$  components of the dipole integrals enter into the transition dipole moment expressions.

TABLE I. Parameters (in eV) of the core- $\sigma_{\text{rad}}$  model Hamiltonian for *p*-, *m*-, and *o*-benzyne evaluated using GASSCF(3e,2o;3e,2o) orbitals averaged over all singlet and triplet states. The *x* and *z* components of the transition dipole integrals ( $\mu_{\text{LE/CT}}$ ) in the MO basis are also reported (in au). All computations use the cc-pCVTZ-DK basis and treat scalar relativistic effects with X2C.

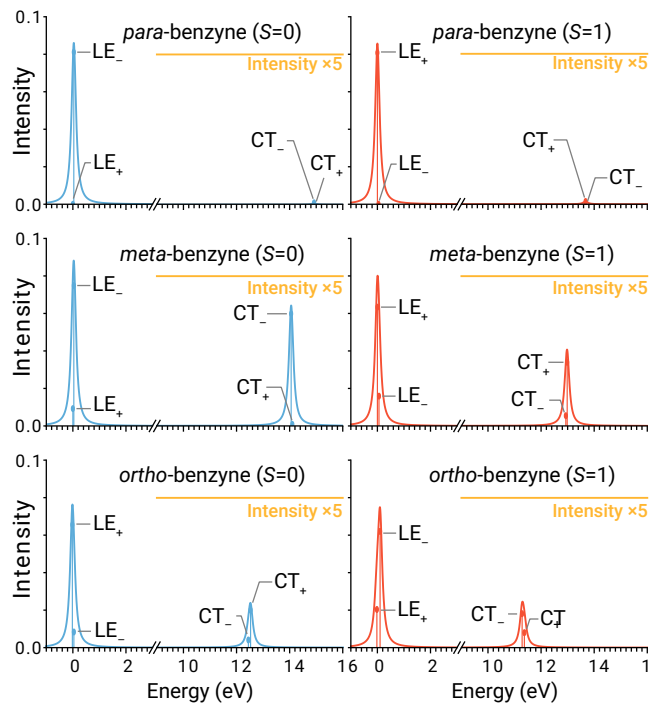
Parameter	<i>para</i>	<i>meta</i>	<i>ortho</i>
$E_{\text{CT}} - E_{\text{LE}}$	14.227	13.097	11.006
$V_{\psi}$	0.584	-1.620	-2.198
$V_{1s}$	0.124	-0.099	-0.116
$K$	0.625	0.641	0.723
$V_{\psi}/(E_{\text{CT}} - E_{\text{LE}})$	0.041	-0.124	-0.200
$\mu_{\text{LE}}^x$	0.076	0.070	-0.035
$\mu_{\text{CT}}^x$	0.001	-0.012	-0.018
$\mu_{\text{LE}}^z$	0.000	-0.032	-0.068
$\mu_{\text{CT}}^z$	0.000	-0.013	0.003

### III. COMPUTATIONAL RESULTS

115

Next, we use our model to predict and assign the basic features of the carbon K-edge spectrum of the benzyne that arise from the radical orbitals. The molecular orbital diagram for the three isomers of benzyne are shown in Fig. S1 of the Supplementary Material. We use GASSCF(3e,2o;3e,2o) orbitals optimized for the average energy of all singlet and triplet core-excited states, followed by Pipek-Mezey localization<sup>37</sup> of the two core and two  $\sigma$  radical orbitals ( $\sigma_{\text{rad}}$ ). We consider a minimal GAS configuration interaction (GASCI) wave function that contains two spaces: 1) a GAS1 for the two localized core orbitals, and 2) a GAS2 for the two localized radical orbitals. For the *para*, *meta*, and *ortho* isomers the two localized  $\sigma_{\text{rad}}$  orbitals correspond to the symmetric and antisymmetric linear combinations of the (5b<sub>1u</sub>, 6a<sub>g</sub>), (11a<sub>1</sub>, 7b<sub>2</sub>), and (10a<sub>1</sub>, 8b<sub>2</sub>) orbitals, respectively. The main purpose of this localization scheme is to aid in the interpretation of the system and it has no impact 120 on the GASCI energies (and the subsequent correlated computations). This GAS generates the same determinant space considered in our model, and from the Hamiltonian in this basis, we extract the corresponding parameters, which are reported in Table I. It is important to note that 125 the computed coupling parameters are directly extracted from *ab initio* calculations. In principle

130 it is possible to extract the Hamiltonian parameters from *ab initio* energies; however, since this problem is ill-posed, we found that it is possible to extract only the LE and CT state energies ( $E_{\text{LE}}$  and  $E_{\text{CT}}$ ) and the exchange integral  $K$ .



135 FIG. 3. Minimum model of the  $\text{C } 1\text{s} \rightarrow \sigma_{\text{rad}}$  X-ray absorption spectrum for the singlet (left) and triplet (right) states of the *o*-, *m*-, and *p*-benzene diradicals computed at the GACI level of theory with a cc-pCVTZ-DK basis set and localized orbitals averaged over singlet and triplet core-excited states. Lorentzian convolution with a line broadening of 0.2 eV (scaled down by a factor of 3) is applied to each spectrum. Intensities for localized excitation and charge transfer transitions are labeled ( $\text{LE}_{\pm}$ ) and ( $\text{CT}_{\pm}$ ), respectively. Intensities for charge-transfer excitations are scaled up by a factor of 5.

140 The GACI spectra of the benzene isomers computed with a six electron in four orbitals active space are shown in Fig. 3. For each molecule, we also assign each transition to the core-excited state predicted by our model. The first molecule we analyze is *p*-benzene, the isomer with radical centers farthest apart (2.744 Å). This singlet ground state of this molecule has the highest diradical character among all the benzenes, and the lowest triplet state lies less than 4 kcal mol<sup>-1</sup> above it.<sup>21</sup> As a consequence, this case falls in the limit of a pure covalent diradical ( $|C_{\text{C}}| \approx 1$ ). As predicted by 145 our model, the LE and CT states form two distinct peaks separated by  $\Delta_S = E_{\text{CT}} + K - E_{\text{LE}} \approx 14.9$  eV. Due to the small value of the coupling  $|V_{\psi} \pm V_{1\text{s}}|$  compared to  $\Delta_S$ , there is small mixing

between the LE and CT configurations in the final states. The splitting within the LE and CT states (proportional to the  $V_{1s}V_{\psi}$  product) is unnoticeable ( $< 0.02$  eV). More importantly, in *p*-benzyne, due to the symmetry of the radical orbitals, only two of the transitions in the singlet and the triplet manifolds are allowed. In the singlet state, even though the transition to  $|CT_+\rangle$  is allowed by symmetry, the small value of  $\mu_{CT}^z$  ( $< 10^{-3}$ ) and the negligible intensity borrowing lead to a near-zero intensity, making this transition hard to resolve on the scale of the spectrum. The triplet spectrum of *p*-benzyne display identical features, showing only one dominant LE peak.

150

155

160

165

170

175

Notable spectral trends appear in *m*-benzyne as the radical centers are closer. Due to changes in symmetry and distance between the radical centers, we observe a tripling of the coupling between the radical MOs ( $V_{\psi}$ ) and a twenty-fold increase in the magnitude of the CT transition dipole ( $\mu_{CT}^x \approx \mu_{CT}^z \approx -0.012$ ). Moreover, the singlet ground state acquires partial zwitterionic character ( $|C_Z| \approx 0.252$ ). As a consequence, three significant changes appear in the singlet core-excitation spectrum. Firstly, compared to *p*-benzyne, the CT state is stabilized by the smaller charge separation of the radical centers, leading to a smaller splitting between the LE and CT states. Secondly, the  $|LE_+\rangle$  state becomes bright, but it is practically indistinguishable from the more intense transition to  $|LE_-\rangle$ . Thirdly, the  $|CT_-\rangle$  state acquires considerable intensity, due to the increase in the magnitude of the transition dipole moments and intensity borrowing, while the  $|CT_+\rangle$  is practically dark. Still, the CT transitions are a factor of at least five less intense than the most intense transition  $|LE_-\rangle$ . These changes are mirrored in the spectrum of the triplet state.

Some of the trend observed for *p*- and *m*-benzyne continue in the *ortho* isomer. The singlet ground state of this isomer has the least diradical character and a sizable singlet-triplet splitting (about 37.5 kcal/mol = 1.63 eV)<sup>21</sup>. The singlet core-excited state spectrum shows a smaller splitting between the LE and CT peaks, due to the decrease of  $E_{CT} - E_{LE}$  (11.0 eV) as charge separation in the CT determinants becomes smaller. Our model shows that an important factor contributing to the variation in the transition dipole moments is intensity borrowing of the CT states due to mixing with the LE determinants. At the lowest order, this mixing is approximately controlled by the prefactor  $\chi = |V_{\psi}|/(E_{CT} - E_{LE})$  (reported in Table I), where we ignore the effect of  $V_{1s}$  in the numerator and of  $K$  in the denominator since they are at least one order of magnitude smaller than  $V_{\psi}$  and  $E_{CT} - E_{LE}$ , respectively. The close proximity of radical centers in *m*- and *o*-benzyne makes this prefactor significant in magnitude (0.124 and 0.200, respectively). The effects of intensity borrowing are most notable in the *ortho* isomer, where together with phase cancellation, it leads to quenching of the intensity of the  $LE_-/CT_-$  and  $LE_+/CT_+$  transitions in the singlet and triplet

spectra, respectively.

180 Our model captures the basic features of the X-ray spectrum of the benzenes that arise from the orbitals on the radical centers. However, it neglects two important effects: 1) dynamical electron correlation and 2) transitions involving other core orbitals and the valence  $\pi$  orbitals. We first examine the effect of dynamical electron correlation by augmenting the GSCI treatment of the 185 diradical core-excited states with third-order perturbative corrections from the driven similarity renormalization group (see Computational Details section in the Supplementary Material).<sup>13,38</sup> Our recent benchmark study<sup>33</sup> has shown that this third-order correction is essential to accurately 190 describe the core-excited state of organic molecules, avoiding possible intruder states and root-flipping. The results computed at this level of theory using the minimal GAS, are shown in the first and third panels of Fig. 4. Dynamical electron correlation does not introduce substantial changes in the spectra of the benzenes. The only noticeable difference is a reduction of the gap between the LE and CT states for all isomers. This effect is consistent with the stabilization of charge-transfer states due to dynamical correlation, as observed in other contexts.<sup>39</sup>

195 Finally, we extend our correlated computations to account for all carbon 1s orbitals and valence  $\pi/\pi^*$  orbitals (shown in Fig. S1 of the Supplementary Material). The second and fourth panels of Fig. 4 show the computed X-ray absorption spectra with this expanded active space. To unravel 200 these more complicated spectra, we analyzed the determinantal composition of the final states, representing lines arising from different sets of C 1s orbitals using different colors and labeling the states that arise from the radicals orbitals with the labels LE and CT. In all the spectra, the lowest energy transitions correspond to LE core excitations  $1s \rightarrow \sigma_{\text{rad}}$ . The corresponding CT states are red-shifted compared to the results from the minimal GAS. This effect is particularly important for *p*- and *m*-benzyne, where the CT states overlap with other transitions. The additional peaks in the expanded GAS spectra correspond to transitions from 1s core orbitals to the  $\pi/\pi^*$  orbitals. Several of these transitions have multi-electron character; for example, they may involve the promotion of two electrons (one from a 1s core and one from a  $\pi$  orbital) to the  $\pi^*$  and  $\sigma_{\text{rad}}$  orbitals.

#### 205 IV. DISCUSSION AND CONCLUSION

Lastly, we discuss the experimental implications of our study. Our model identifies the emergence of two groups of transitions to localized and charge-transfer states as one of the major features of the spectrum of diradicals. The locality of the transition dipole integrals leads to quenching of charge-transfer excitations, which in the X-ray spectra of the benzenes are weak and cannot be

210 distinguished from other transitions involving  $\pi$  orbitals. Under our model, the singlet and triplet  
215 LE core-excited states are near degenerate (due to a vanishing exchange integral), implying that  
the ground state singlet-triplet splitting is reflected in the different frequencies of these transitions.  
Another property of the ground state that impacts the X-ray spectrum is the degree of mixing of  
220 covalent and zwitterionic configurations in the singlet ground state. However, the covalent character  
of the ground state cannot be easily inferred from the X-ray spectrum since the impact of this  
225 quantity on peak intensities is modulated by the degree of LE/CT configuration mixing (intensity  
borrowing) and the magnitude of the transition dipole integrals. Our analysis suggests that no other  
features of the core-excited state spectrum allow directly extracting quantitative information about  
the ground state (energies, exchange integrals).

230 In summary, we proposed a simple theoretical model of the core-excited states of diradical  
species and used it to explain the features of the X-ray absorption spectra of the three isomers  
235 of benzyne. Our model demonstrates the breakdown of an independent particle view in the  
core-excited states of diradicals, with many-body interactions leading to highly entangled states  
that display heavy electronic configuration mixing. Using our model, we clarified the connection  
between the ground-state electronic structure of diradicals and their X-ray spectral features (relative  
transition energies and intensities). In particular, we were able to unravel the contributions of  
the radical carbon atoms in the spectra of the benzyne. To the best of our knowledge, there  
are no measurements of the carbon K-edge spectrum of the benzyne; therefore, our theoretical  
predictions might be useful to guide future XAS experiments targeting these molecules. The model  
we presented focuses on symmetric systems with two valence open-shell electrons. However, it  
can be easily generalized to more than two valence open-shell electrons or to systems with more  
than two radical centers. In this case, the determinant basis will still be composed of localized and  
charge-transfer excitations, but it would rapidly grow in size (combinatorially) with the number  
240 of valence orbitals and unpaired electrons. These extension would make our model applicable  
to non-symmetric diradicals and complexes containing two transition metal atoms,<sup>40</sup> where the  
mixing of metal d orbitals and ligand orbitals could lead to new spectral features.

## ACKNOWLEDGMENTS

245 This research was supported by the U.S. National Science Foundation under award number  
CHEM-1900532 and by a Camille Dreyfus Teacher-Scholar Award (No. TC-18-045).

240

**SUPPLEMENTARY MATERIAL**

245

The supplementary material includes: 1) equations for the transition dipole moments, 2) details of the DSRG-MRPT3 computations of the X-ray absorption spectra of the benzenes, 3) the molecular orbital diagram of the benzenes and GAS spaces used in the DSRG-MRPT3 computations , 4) the Cartesian geometries of the benzenes, and 5) excitation energies and absorption intensities computed at the DSRG-MRPT3 level with the expanded GAS.

250

255

260

265

**REFERENCES**

- <sup>1</sup>P. Norman and A. Drew, *Chem. Rev.* **118**, 7208 (2018).
- <sup>2</sup>A. Iglesias-Juez, G. L. Chiarello, G. S. Patience, and M. O. Guerrero-Pérez, *Can. J. Chem. Eng.* **100**, 3 (2022).
- <sup>3</sup>H. Ågren, V. Carravetta, O. Vahtras, and L. G. M. Pettersson, *Chem. Phys. Lett.* **222**, 75 (1994).
- <sup>4</sup>A. T. B. Gilbert, N. A. Besley, and P. M. W. Gill, *J. Phys. Chem. A* **112**, 13164 (2008).
- <sup>5</sup>W. D. Derricotte and F. A. Evangelista, *Phys. Chem. Chem. Phys.* **17**, 14360 (2015).
- <sup>6</sup>K. J. Oosterbaan, A. F. White, and M. Head-Gordon, *J. Chem. Phys.* **149**, 044116 (2018).
- <sup>7</sup>M. Simons and D. A. Matthews, *J. Chem. Phys.* **154**, 014106 (2021), 2011.03595.
- <sup>8</sup>R. H. Myhre, T. J. A. Wolf, L. Cheng, S. Nandi, S. Coriani, M. Gühr, and H. Koch, *J. Chem. Phys.* **148**, 064106 (2018).
- <sup>9</sup>R. C. Couto, L. Kjellsson, H. Ågren, V. Carravetta, S. L. Sorensen, M. Kubin, C. Bülow, M. Timm, V. Zamudio-Bayer, B. v. Issendorff, J. T. Lau, J. Söderström, J.-E. Rubensson, and R. Lindblad, *Phys. Chem. Chem. Phys.* **22**, 16215 (2020).
- <sup>10</sup>M. Epshtain, V. Scutelnic, Z. Yang, T. Xue, M. L. Vidal, A. I. Krylov, S. Coriani, and S. R. Leone, *J. Phys. Chem. A* **124**, 9524 (2020).
- <sup>11</sup>M. Roemelt, D. Maganas, S. DeBeer, and F. Neese, *J. Chem. Phys.* **138**, 204101 (2013).
- <sup>12</sup>D. Hait, E. A. Haugen, Z. Yang, K. J. Oosterbaan, S. R. Leone, and M. Head-Gordon, *J. Chem. Phys.* **153**, 134108 (2020).
- <sup>13</sup>M. Huang, C. Li, and F. A. Evangelista, *J. Chem. Theory Comput.* **18**, 219 (2022).
- <sup>14</sup>M. L. Vidal, M. Epshtain, V. Scutelnic, Z. Yang, T. Xue, S. R. Leone, A. I. Krylov, and S. Coriani, *J. Phys. Chem. A* **124**, 9532 (2020).
- <sup>15</sup>F. Neese, B. Hedman, K. O. Hodgson, and E. I. Solomon, *Inorg. Chem.* **38**, 4854 (1999).

<sup>16</sup>R. Lindblad, L. Kjellsson, R. C. Couto, M. Timm, C. Bülow, V. Zamudio-Bayer, M. Lundberg,  
270 B. Von Issendorff, J. Lau, S. Sorensen, *et al.*, Phys. Rev. Lett. **124**, 203001 (2020).

<sup>17</sup>M. Abe, Chem. Rev. **113**, 7011 (2013).

<sup>18</sup>T. Stuyver, B. Chen, T. Zeng, P. Geerlings, F. De Proft, and R. Hoffmann, Chem. Rev. **119**,  
11291 (2019).

<sup>19</sup>R. Marquardt, W. Sander, and E. Kraka, Angew. Chem., Int. Ed. **35**, 746 (1996).

<sup>275</sup><sup>20</sup>P. G. Wenthold, J. Hu, and R. R. Squires, J. Am. Chem. Soc. **118**, 11865 (1996).

<sup>21</sup>P. G. Wenthold, R. R. Squires, and W. C. Lineberger, J. Am. Chem. Soc. **120**, 5279 (1998).

<sup>22</sup>A. Chrostowska, G. Pfister-Guillouzo, F. Gracian, and C. Wentrup, Aust. J. Chem. **63**, 1084  
(2010).

<sup>280</sup><sup>23</sup>D. Kaiser, E. Reusch, P. Hemberger, A. Bodi, E. Welz, B. Engels, and I. Fischer, Phys. Chem. Chem. Phys. **20**, 3988 (2018).

<sup>24</sup>M. Gerlach, E. Karaev, D. Schaffner, P. Hemberger, and I. Fischer, J. Phys. Chem. Lett. **13**,  
11295–11299 (2022).

<sup>25</sup>C. J. Cramer, J. J. Nash, and R. R. Squires, Chem. Phys. Lett. **277**, 311 (1997).

<sup>26</sup>T. D. Crawford, E. Kraka, J. F. Stanton, and D. Cremer, J. Chem. Phys. **114**, 10638 (2001).

<sup>285</sup><sup>27</sup>E. B. Wang, C. A. Parish, and H. Lischka, J. Chem. Phys. **129**, 044306 (2008).

<sup>28</sup>W. A. Al-Saidi and C. J. Umrigar, J. Chem. Phys. **128**, 154324 (2008), 0803.0946.

<sup>29</sup>S. E. Smart, J.-N. Boyn, and D. A. Mazziotti, Phys. Rev. A **105**, 022405 (2022).

<sup>30</sup>C. E. de Moura and A. Y. Sokolov, Phys. Chem. Chem. Phys. **24**, 4769 (2022).

<sup>31</sup>Y. Shao, M. Head-Gordon, and A. I. Krylov, J. Chem. Phys. **118**, 4807 (2003).

<sup>290</sup><sup>32</sup>L. V. Slipchenko and A. I. Krylov, J. Chem. Phys. **117**, 4694 (2002).

<sup>33</sup>M. Huang and F. Evangelista, “A benchmark study of core-excited states of organic molecules  
computed with the generalized active space driven similarity renormalization group,” (2022).

<sup>34</sup>R. J. Cave and M. D. Newton, Chem. Phys. Lett. **249**, 15 (1996).

<sup>35</sup>J. E. Subotnik, S. Yeganeh, R. J. Cave, and M. A. Ratner, J. Chem. Phys. **129**, 244101 (2008).

<sup>295</sup><sup>36</sup>M. B. Smith and J. Michl, Chem. Rev. **110**, 6891 (2010).

<sup>37</sup>J. Pipek and P. G. Mezey, J. Chem. Phys. **90**, 4916 (1989).

<sup>38</sup>C. Li and F. A. Evangelista, J. Chem. Phys. **146**, 124132 (2017).

<sup>39</sup>L. Serrano-Andres, R. Lindh, B. O. Roos, and M. Merchan, J. Phys. Chem. **97**, 9360–9368  
(1993).

This is the author's peer reviewed, accepted manuscript. However, the online version of record will be different from this version once it has been copyedited and typeset.  
PLEASE CITE THIS ARTICLE AS DOI: 10.1063/5.0140761

300 <sup>40</sup>M. W. Mara, B. T. Phelan, Z.-L. Xie, T. W. Kim, D. J. Hsu, X. Liu, A. J. Valentine, P. Kim, X. Li, S.-i. Adachi, *et al.*, *Chem. Sci.* **13**, 1715 (2022).

This is the author's peer reviewed, accepted manuscript. However, the online version of record will be different from this version once it has been copyedited and typeset.  
PLEASE CITE THIS ARTICLE AS DOI: 10.1063/5.0140761

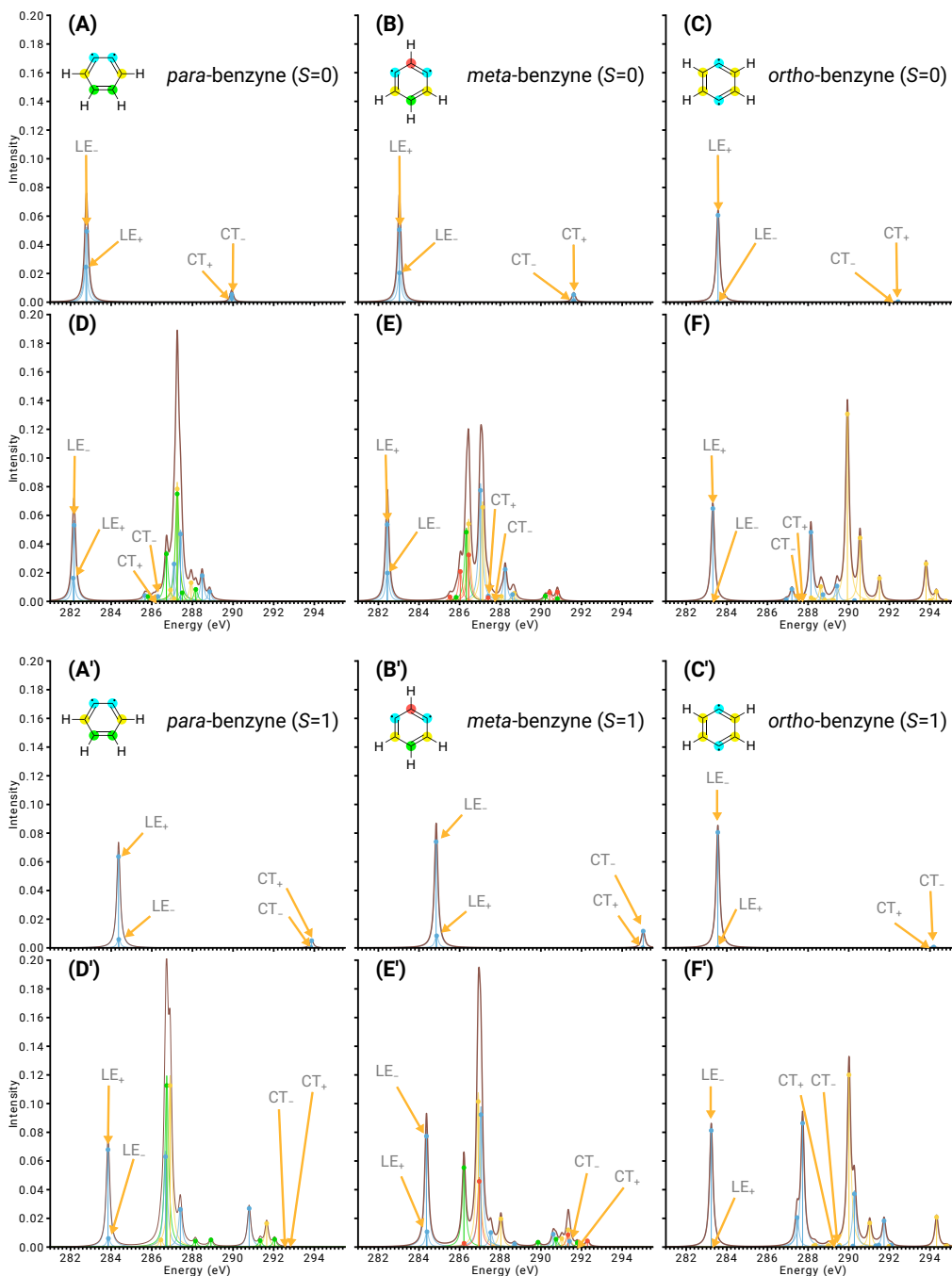


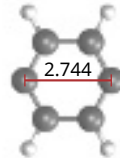
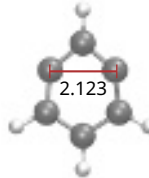
FIG. 4. Carbon K-edge absorption spectrum of singlet (A, D) *ortho*-, (B, E) *meta*-, and (C, F) *para*-benzene computed with a minimal (C 1s  $\rightarrow$   $\sigma_{\text{rad}}$ , top) and expanded (C 1s  $\rightarrow$   $\pi_{1-6}\sigma_{\text{rad}}$ , bottom) GAS at the DSRG-MRPT3 level of theory and a cc-pCVQZ-DK basis set. Peaks are color-coded based on the carbon core orbital involved in the transition. A Lorentzian convolution with a line broadening of 0.2 eV (scaled down by a factor of 3) is applied to each spectra. Intensities for localized excitation and charge transfer transitions are labeled (LE $\pm$ ) and (CT $\pm$ ), respectively.

Accepted to *J. Chem. Phys.*

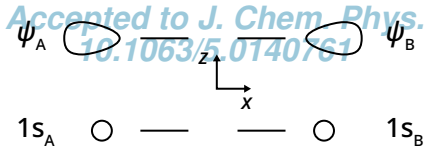
1.277

10.1

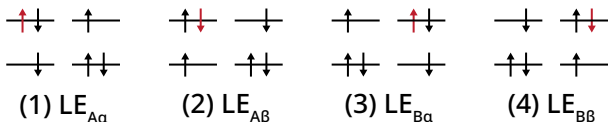
761



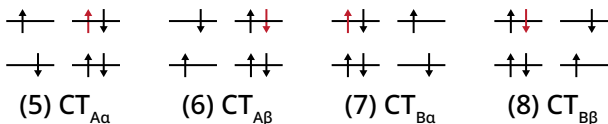
$x$   
 $y$   
 $z$

**A****B**

Determinant basis for local excitations (LE)



Determinant basis for charge-transfer excitations (CT)

**C**